J|A|C|S ARTICLES

Published on Web 03/26/2009

Investigation of the Catalytic Mechanism of a Synthetic DNAzyme with Protein-like Functionality: An RNaseA Mimic?

Jason M. Thomas, Jung-Ki Yoon, and David M. Perrin*

Department of Chemistry, University of British Columbia, 2036 Main Mall, Vancouver, British Columbia, Canada V6T 1Z1

Received January 7, 2009; E-mail: dperrin@chem.ubc.ca

Abstract: The protein enzyme ribonuclease A (RNaseA) cleaves RNA with catalytic perfection, although with little sequence specificity, by a divalent metal ion (M^{2+})-independent mechanism in which a pair of imidazoles provides general acid and base catalysis, while a cationic amine provides electrostatic stabilization of the transition state. Synthetic imitation of this remarkable organo-catalyst ("RNaseA mimicry") has been a longstanding goal in biomimetic chemistry. The 9_{25}-11 DNAzyme contains synthetically modified nucleotides presenting both imidazole and cationic amine side chains, and catalyzes RNA cleavage with turnover in the absence of M^{2+} similarly to RNaseA. Nevertheless, the catalytic roles, if any, of the "protein-like" functional groups have not been defined, and hence the question remains whether 9_{25}-11 engages any of these functionalities to mimic aspects of the mechanism of RNaseA. To address this question, we report a mechanistic investigation of 9_{25}-11 catalysis wherein we have employed a variety of experiments, such as DNAzyme functional group deletion, mechanism-based affinity labeling, and bridging and nonbridging phosphorothioate substitution of the scissile phosphate. Several striking parallels exist between the results presented here for 9_{25}-11 and the results of analogous experiments applied previously to RNaseA. Specifically, our results implicate two particular imidazoles in general acid and base catalysis and suggest that a specific cationic amine stabilizes the transition state via diastereoselective interaction with the scissile phosphate. Overall, 9_{25}-11 appears to meet the minimal criteria of an RNaseA mimic; this demonstrates how added synthetic functionality can expand the mechanistic repertoire available to a synthetic DNA-based catalyst.

Introduction

The protein enzyme RNaseA catalyzes RNA cleavage to yield 2′,3′-cyclic phosphodiester and 5′-hydroxyl-terminated products.[1] RNaseA has achieved catalytic perfection in that diffusion-controlled substrate association has been shown to be the rate-limiting step in catalysis.[2] The active site which delivers this remarkable degree of transition-state stabilization is depicted in Scheme 1; therein, the imidazole side chains of His119 and His12 are the general acid and the general base, respectively.[1,3] The cationic amine side chain of Lys41 is also believed to provide electrostatic/hydrogen bond stabilization of the developing negative charge on the nonbridging scissile phosphate oxygens in the transition state.[4] It is particularly noteworthy that RNaseA catalyzes RNA cleavage without the assistance of a divalent metal cation (M^{2+}) cofactor. In contrast, M^{2+}-mediated catalysis is a common strategy in many other phosphodiester transfer or hydrolysis catalysts, be they protein enzymes, catalytic nucleic acids, or synthetic constructs.[5] In light of having evolved to catalytic perfection in the absence of a M^{2+}, RNaseA represents a venerable example of the power of organo-catalysis at the enzymatic level.

Scheme 1. Simplified Rendering of the Active Site Catalytic Mechanism of RNaseA[1−3]

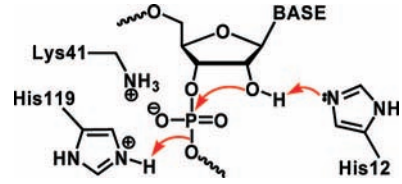

The design of synthetic catalysts that imitate RNaseA has been pursued both to provide fundamental mechanistic insight and to meet a formidable challenge of artificial enzyme design in the fields of biomimetic chemistry and organo-catalysis.[6,7] Efforts toward RNaseA mimicry in synthetic catalysts have generally involved the conjugation of imidazole, amine, guanidinine, or related functionalities to a variety of scaffolds; designs

(1) Raines, R. T. *Chem. Rev.* **1998**, *98*, 1045–1065.
(2) Park, C.; Raines, R. T. *Biochemistry* **2003**, *42*, 3509–3518.
(3) Thompson, J. E.; Raines, R. T. *J. Am. Chem. Soc.* **1994**, *116*, 5467–5468.
(4) Messmore, J. M.; Fuchs, D. N.; Raines, R. T. *J. Am. Chem. Soc.* **1995**, *117*, 8057–8060.
(5) (a) Steitz, T. A.; Steitz, J. A. *Proc. Natl. Acad. Sci. U.S.A.* **1993**, *90*, 6498–6502. (b) Trawick, B. N.; Daniher, A. T.; Bashkin, J. K. *Chem. Rev.* **1998**, *98*, 939–960. (c) Hanna, R.; Doudna, J. A. *Curr. Opin. Chem. Biol.* **2000**, *4*, 166–170. (d) Neverov, A. A.; Lu, Z.-L.; Maxwell, C. I.; Mohamed, M. F.; White, C. J.; Tsang, J. S. W.; Brown, R. S. *J. Am. Chem. Soc.* **2006**, *128*, 16398–16405. (e) Bunn, S. E.; Liu, C. T.; Lu, Z.-L.; Neverov, A. A.; Brown, R. S. *J. Am. Chem. Soc.* **2007**, *129*, 16238–16248. (f) Sigel, R. K. O.; Pyle, A. M. *Chem. Rev.* **2007**, *107*, 97–113. (g) Yang, W. *Nat. Struct. Biol.* **2008**, *15*, 1228–123. (h) Liu, C. T.; Neverov, A. A.; Brown, R. S. *J. Am. Chem. Soc.* **2008**, *130*, 16711–16720.
(6) Breslow, R. *Acc. Chem. Res.* **1991**, *24*, 317–324.
(7) Breslow, R. *Acc. Chem. Res.* **1995**, *28*, 146–153.

10.1021/ja900125n CCC: $40.75

have ranged from low-molecular-weight organic compounds[8,9] to larger scaffolds such as cyclodextrins and peptides.[6,7,10] In some cases, M^{2+}-independent cleavage of RNA or model phosphodiester substrates has been demonstrated; however, these types of synthetic catalysts generally lack sequence specificity, which is essential for potential biotechnological/medicinal applications. Sequence specificity has been conferred upon these synthetic organo-catalysts by appending oligonucleotide or PNA "guide sequences",[11] which provide base-pairing interactions to direct the catalytic activity specifically to the intended RNA target site. Because most, if not all of the binding energy is therefore ground-state derived, product release is likely to be slow. Indeed, we are not aware of any example where multiple turnover has been demonstrated in the presence of excess substrate.

DNAzymes and ribozymes cleave RNA with both high sequence specificity and reasonably efficient catalytic turnover in some cases. Nevertheless, the catalytic power (k_{cat}/k_{uncat}) of most nucleic acid catalysts falls far short of that of RNaseA. Moreover, for optimal activity, nucleic acid catalysts usually require M^{2+} concentrations (usually 5−25 mM where $M^{2+} = Mg^{2+}$)[12] which greatly exceeded physiological levels (<0.5 mM for Mg^{2+}).[13] While the precise role of M^{2+} in catalysis has been hotly debated, the common M^{2+}-dependence and general catalytic inferiority of nucleic acid catalysts with respect to RNA cleavage have been attributed, in part, to the absence of a nitrogenous cation (e.g., ammonium, guanidinium) as well as an imidazole which is ideally suited for general acid/base catalysis at physiological pH.[14] Given these perceived shortcomings in catalytic nucleic acids, an enduring interest in synthetic sequence-specific RNaseA mimics persists.

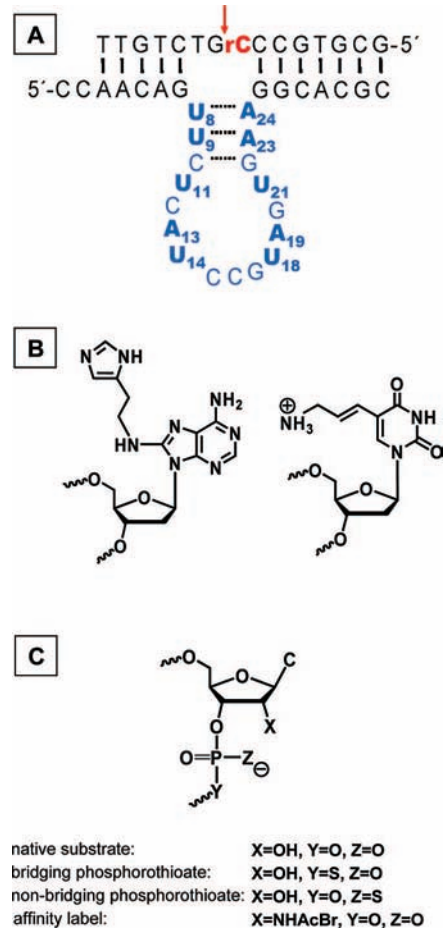

Figure 1. (A) The 9_{25}-11 DNAzyme in complex with substrate. The substrate cleavage site at the embedded ribo-C (red) is indicated by the arrow; the catalytic stem loop of 9_{25}-11 (blue) is numbered from the 5-terminus of the DNAzyme strand. (B) The modified nucleotides incorporated into 9_{25}-11: 8-histaminyl-deoxyadenosine (^{his}dA) and 5-aminoallyl-deoxyuridine (^{aa}dU); these nucleotides are indicated in panel (A) as bold **A** and **U**. (C) The cleavage site nucleotide in the substrates and analogues used in this study.

In an effort to integrate the desirable properties of sequence specificity (characteristic of DNAzymes and ribozymes) and M^{2+}-independent catalysis (characteristic of RNaseA), the 9_{25}-11 DNAzyme (Figure 1A) was discovered[15] by combinatorial *in vitro* selection (SELEX),[16] wherein two of the natural DNA monomers were replaced with analogues bearing imidazoles and cationic amines. Underlying this work was the hypothesis that the catalytic inferiority of RNA-cleaving nucleic acid catalysts in the absence of M^{2+} cations at physiological ionic strength could be alleviated by endowing them with RNaseA-like

(8) Scheffer, U.; Strick, A.; Ludwig, V.; Peter, S.; Kalden, E.; Göbel, M. W. *J. Am. Chem. Soc.* **2005**, *127*, 2211–2217.
(9) Orth, E. S.; Branda, T. A. S.; Milagre, H. M. S.; Eberlin, M. N.; Nome, F. *J. Am. Chem. Soc.* **2008**, *130*, 2436–2437.
(10) Razkin, J.; Nilsson, H.; Baltzer, L. *J. Am. Chem. Soc.* **2007**, *129*, 14752–14758.
(11) (a) Komiyama, M.; Inokawa, T.; Yoshinari, K. *Chem. Commun.* **1995**, 77–78. (b) Shinozuka, K.; Umeda, A.; Ozaki, H.; Sawai, H. *Nucleic Acids Symp. Ser.* **1996**, *35*, 121–122. (c) Endo, M.; Azuma, Y.; Saga, Y.; Kuzuya, A.; Kawai, G.; Komiyama, M. *J. Org. Chem.* **1997**, *62*, 846–852. (d) Verheijen, J. C.; Deiman, B. A. L. M.; Yeheskiely, E.; van der Marel, G. A.; van Boom, J. H. *Angew. Chem.* **2000**, *39*, 369–372. (e) Petersen, L.; de Koning, M. C.; van Kuik-Romeijn, P.; Weterings, J.; Pol, C. J.; Platenburg, C.; Beloglazova, N. G.; Silnikov, V. N.; Zenkowa, M. A.; Vlassov, V. V. *FEBS Lett.* **2000**, *481*, 277–280. (f) Verbeure, B.; Lacey, C. J.; Froeyen, M.; Rozenski, J.; Herdewijn, P. *Bioconjugate Chem.* **2002**, *13*, 333–350. (g) Overhand, M.; van der Marel, G. A.; van Boom, J. H. *Bioconjugate Chem.* **2004**, *15*, 576–582. (h) Beloglazova, N. G.; Fabani, M. M.; Zenkova, M. A.; Bichenkova, E. V.; Polushin, N. N.; Silnikov, V. N.; Douglas, K. T.; Vlassov, V. V. *Nucleic Acids Res.* **2004**, *32*, 3887–3897. (i) Gnaccarini, C.; Peter, S.; Scheffer, U.; Vonhoff, S.; Klussmann, S.; Göbel, M. W. *J. Am. Chem. Soc.* **2006**, *128*, 8063–8067.
(12) Reasonably efficient catalytic activity has been reported in some cases for nucleic acid catalysts in the absence of divalent metal cations, but at high (molar) monovalent cation concentrations or in the presence of polyamines or exchange inert $Co(NH_3)^{3+}$. For example: (a) Geyer, C. R.; Sen, D. *Chem. Biol.* **1997**, *4*, 579–593. (b) Hampel, A.; Cowan, J. A. *Chem. Biol.* **1997**, *4*, 513–517. (c) Nesbitt, S.; Hegg, L. A.; Fedor, M. J. *Chem. Biol.* **1997**, *4*, 619–630. (d) Young, K. J.; Gill, F.; Grasby, J. A. *Nucleic Acids Res.* **1997**, *25*, 3760–3766. (e) Earnshaw, D. J.; Gait, M. J. *Nucleic Acids Res.* **1998**, *26*, 5551–5561. (f) Murray, J. B.; Seyhan, A. A.; Walter, N. G.; Burke, J. M.; Scott, W. G. *Chem. Biol.* **1998**, *5*, 587–595. (g) Nakano, S.-I.; Chadalavada, D. M.; Bevilacqua, P. C. *Science* **2000**, *287*, 1493–1497. (h) O'Rear, J. L.; Wang, S.; Feig, A. L.; Beigelman, L.; Uhlenbeck, O. C.; Herschlag, D. *RNA* **2001**, *7*, 537–545. (i) Curtis, E. A.; Bartel, D. P. *RNA* **2001**, *7*, 546–552. (j) Carrigan, M. A.; Ricardo, A.; Ang, D. N.; Benner, S. A. *Biochemistry* **2004**, *43*, 11446–11459. (k) Cerrone-Szakal, A. L.; Siegfried, N. A.; Bevilacqua, P. C. *J. Am. Chem. Soc.* **2008**, *130*, 14504–14520.
(13) (a) Mulquiney, P. J.; Kuchel, P. W. *NMR Biomed.* **1997**, *10*, 129–137. (b) Murphy, E.; Freudenrich, C. C.; Levy, L. A.; London, R. E.; Lieberman, M. *Proc. Natl. Acad. Sci. U.S.A.* **1989**, *86*, 2981–2984. (c) Murphy, E.; Steenbergen, C.; Levy, L. A.; Raju, B.; London, R. E. *J. Biol. Chem.* **1989**, *264*, 5622–5627. (d) Suzuki, Y.; Komatsu, H.; Ikeda, T.; Saito, N.; Araki, S.; Citterio, D.; Hisamoto, H.; Kitamura, Y.; Kubota, T.; Nakagawa, J.; Oka, K.; Suzuki, K. *Anal. Chem.* **2002**, *74*, 1423–1428.
(14) Narlikar, G. J.; Herschlag, D. *Annu. Rev. Biochem.* **1997**, *66*, 19–59.
(15) Perrin, D. M.; Garestier, T.; Helene, C. *J. Am. Chem. Soc.* **2001**, *123*, 1556–1563.
(16) (a) Tuerk, C.; Gold, L. *Science* **1990**, *249*, 505–510. (b) Ellington, A. D.; Szostak, J. W. *Nature* **1990**, *346*, 818–822. (c) Breaker, R. R.; Joyce, G. F. *Chem. Biol.* **1994**, *1*, 223–229.

functionality. We tested this hypothesis by selecting for M^{2+}-independent ribonuclease activity, and in so doing we also addressed the specific challenge of developing RNaseA mimics through a combinatorial approach, as opposed to rational design.

Although the hypothetical 2D structure of the 9_{25}-11 DNAzyme is similar to those of other small ribozymes and DNAzymes, 9_{25}-11 is functionally similar to synthetic RNaseA mimics by virtue of its 10 unnatural modified bases: four 8-histaminyl-deoxyadenosine (^{his}dA) and six 5-aminoallyl-deoxyuridine (^{aa}dU) residues (Figure 1B). 9_{25}-11 has been shown to cleave an RNA linkage (embedded within a DNA substrate) with high sequence specificity and reasonably efficient turnover, in the absence of a M^{2+}-cofactor ($k_{cat}/K_m \approx 5 \times 10^5\ M^{-1}\ min^{-1}$).[17] However, the chemical basis for catalysis has not been investigated in detail, and the question remains: Is 9_{25}-11 a functional RNaseA mimic? To answer this question, we now report a detailed enzymological characterization of 9_{25}-11 catalysis, to determine if the synthetic modifications indeed play the intended roles in catalysis characteristic of RNaseA, rather than supporting structural roles. Notably, several other synthetically modified nucleic acid catalysts have been discovered by *in vitro* selection,[18] but little subsequent investigation has been reported into the mechanistic roles of the synthetically appended functionalities. Thus, 9_{25}-11 presents a useful test case in which to assess the actual contribution to catalysis of synthetic modifications in a nucleic acid catalyst.

We began this study by verifying that the general aspects of 9_{25}-11 catalysis, such as pH−rate and solvent kinetic isotope effects, are consistent with a general acid/base-catalyzed mechanism. We then probed for specific DNAzyme functional groups involved in active site chemistry using mechanism-based affinity labeling[19−21] and bridging and nonbridging phosphorothioate substrate cleavage experiments (Figure 1C),[22−30] each in the context of DNAzyme functional group deletion. The results of these experiments provide strong evidence for imidazole-mediated general acid and base catalysis, as well as the involvement of a cationic amine in a diastereoselective, transition-state stabilizing interaction with the scissile phosphate. The results presented here for 9_{25}-11 strongly parallel those from analogous mechanistic experiments with RNaseA and provide compelling functional evidence that 9_{25}-11 mimics the active site mechanism of RNaseA. Our findings emphasize the value of synthetic modifications for expanding the mechanistic repertoire of nucleic acid catalysts, in this case to improve DNAzyme-mediated RNA cleavage at low ionic strength in the absence of a M^{2+} cofactor.

Materials and Methods

Chemicals and Biochemicals. All chemicals and buffers salts were purchased from Sigma-Aldrich. Oligonucleotides were synthesized at the University of Calgary DNA Services Laboratory and Trilink Biotech. The preparation of the modified nucleoside phosphoramidites used in the synthesis of 9_{25}-11 has been described in detail elsewhere.[17,31,32] T4 polynucleotide kinase and T4 DNA ligase were purchased from Invitrogen, RNaseA and shrimp alkaline phosphatase from Fermentas, Micrococcal Nuclease from USB, Superase-in RNase inhibitor from Ambion, γ-^{32}P-ATP from Perkin-Elmer, and streptavidin magnetic particles from Roche. Deuterated buffer solutions were prepared by dissolving buffer salts in D_2O (Cambridge Isotopes), adjusting the pH with HCl or NaOH, and then lyophilizing the buffer salts to dryness and resuspending in D_2O four times. The pD was then determined by adding 0.4 to the observed pH-meter reading.[33]

Oligonucleotide Sequences. The originally selected[15] 9_{25}-11 DNAzyme, *trans*-cleaving construct[17] (Figure 1A,B), is referred to as "wildtype 9_{25}-11" in the text: 5′-CCAACAG**UUCUCA**UC-CG**UAGUGAA**GGCACGC, where **A**(bold) is 8-histaminyl-2′-deoxyadenosine (abbreviated as ^{his}dA in the text) and **U**(bold) is 5-aminoallyl-2′-deoxyuridine (abbreviated as ^{aa}dU in the text). 9_{25}-11 functional group deletion variants were synthesized by replacing, one at a time, each ^{his}dA with 8-methylamino-deoxyadenosine[32] or each ^{aa}dU with natural thymidine (see Figure 3, below). These variants are named to reflect the modified nucleotide residue (numbered as in Figure 1A) from which the imidazole or cationic amine was deleted (see Table 1, below). 5′-Product (oligo-**1**), 5′-d(GCGTGCC)**X**, where **X** is ribo-C; 3′-product (oligo-**2**), 5′-d(GTCTGTT); bridging phosphorothioate (S-link) substrate (oligo-**3**), 5′-d(GCGTGCC-**X**-**Y**-TCTGTT), where **Y** is 5′-mercapto-2′,5′-dideoxy-G; native (O-link) substrate (oligo-**4**), 5′-d(GCGTGCC-**X**-GTCTGTT); ligation template (oligo-**5**), 5′-biotin-d(AACAGACGGGCACGC); 2′-amino substrate analogue (oligo-**6**), 5′-d(GCGTGCC-**Z**-GTCTGTTGG), where **Z** is 2′-amino-C; nonbridging phosphorothioate substrate (oligo-**7**), 5′-d(GCGTGCC-**X(sP)**-GTCTGTT), where **X(sP)** represents ribo-C with a 3′-nonbridging phosphorothioate linkage (a ∼50:50 diastereomeric mixture was used). Except for the S-link substrate (oligo-**3**), oligonucleotides were prepared by standard automated synthesis, purified by 7 M urea/TBE PAGE, and desalted as described previously.[34,35]

Kinetic Experiments. Single-turnover cleavage assays were carried out with a saturating excess of 9_{25}-11 (2.5 μM, ∼35 times greater than K_m) and a trace of ^{32}P-labeled substrate (one of oligos-**3**, **4**, or **7**). The standard reaction conditions were 50 mM appropriate buffer, 200 mM NaCl, and 1 mM EDTA at room temperature (21−22 °C). Buffers used were Na-MES (6.82−7.11),

(17) Lermer, L.; Roupioz, Y.; Ting, R.; Perrin, D. M. *J. Am. Chem. Soc.* **2002**, *124*, 9960–9961.
(18) (a) Teramoto, N.; Imanishi, Y.; Ito, Y. *Bioconjugate Chem.* **2000**, *11*, 744–748. (b) Santoro, S. W.; Joyce, G. F.; Sakthivel, K.; Gramatikova, S.; Barbas, C. F. *J. Am. Chem. Soc.* **2000**, *122*, 2433–2439. (c) Sidorov, A. V.; Grasby, J. A.; Williams, D. M. *Nucleic Acids Res.* **2004**, *32*, 1591–1601. (d) Gugliotti, L.; Feldheim, D. L.; Eaton, B. *Science* **2004**, *304*, 850–852. (e) Gugliotti, L. A.; Feldheim, D. L.; Eaton, B. E. *J. Am. Chem. Soc.* **2005**, *127*, 17814–17818. (f) Li, M.; Lin, N.; Huang, Z.; Du, L.; Altier, C.; Fang, H.; Wang, B. *J. Am. Chem. Soc.* **2008**, *130*, 12636–12638. (g) Hollenstein, M; Hipolito, C.; Lam, C.; Dietrich, D.; Perrin, D. M. *Angew. Chem.* **2008**, *47*, 4346–4350.
(19) Hummel, C. F.; Pincus, M. R.; Brandt-Rauf, P. W.; Frei, G. M.; Carty, R. P. *Biochemistry* **1987**, *26*, 135–146.
(20) Thomas, J. M.; Perrin, D. M. *J. Am. Chem. Soc.* **2006**, *128*, 16540–16545.
(21) Thomas, J. M.; Perrin, D. M. *J. Am. Chem. Soc.* **2008**, *130*, 15467–15475.
(22) Thomson, J. B.; Patel, B. K.; Jimenez, V.; Eckart, K.; Eckstein, F. *J. Org. Chem.* **1996**, *61*, 6273–6281.
(23) Hondal, R. J.; Zhao, Z.; Bruzik, K. S.; Tsai, M.-D. *J. Am. Chem. Soc.* **1997**, *119*, 5477–5478.
(24) Hondal, R. J.; Zhao, Z.; Riddle, S. R.; Kravchuk, A. V.; Liao, H.; Bruzik, K. S.; Tsai, M.-D. *J. Am. Chem. Soc.* **1997**, *119*, 9933–9934.
(25) Zhao, L.; Liu, Y.; Bruzik, K. S.; Tsai, M.-D. *J. Am. Chem. Soc.* **2003**, *125*, 22–23.
(26) Das, S. R.; Piccirilli, J. A. *Nat. Chem. Biol.* **2005**, *1*, 45–52.
(27) Thomas, J. M.; Perrin, D. M. *J. Am. Chem. Soc.* **2009**, *131*, 1135–1143.
(28) Herschlag, D. *J. Am. Chem. Soc.* **1994**, *116*, 11631–11635.
(29) Eckstein, F. *FEBS Lett.* **1968**, *2*, 85–86.
(30) Burgers, M. J.; Eckstein, F. *Biochemistry* **1979**, *18*, 592–596.
(31) Lermer, L.; Hobbs, J.; Perrin, D. M. *Nucleosides, Nucleotides, Nucleic Acids* **2002**, *21*, 651–664.
(32) May, J. P.; Ting, R.; Lermer, L.; Thomas, J. M.; Roupioz, Y; Perrin, D. M. *J. Am. Chem. Soc.* **2004**, *126*, 4145–4156.
(33) Schowen, K. B.; Schowen, R. L. *Methods Enzymol.* **1982**, *87*, 551–606.
(34) Ting, R.; Thomas, J. M.; Lermer, L.; Perrin, D. M. *Nucleic Acids Res.* **2004**, *32*, 6660–6672.
(35) Ting, R.; Thomas, J. M.; Perrin, D. M. *Can. J. Chem.* **2007**, *85*, 313–329.

Na-MOPS (7.12−7.35), Na-HEPES (pH 7.35−7.82), Tris-HCl (pH 7.82−8.67), and Na-borate (8.68−9.0). Buffer-specific counterion effects were minimal, as similar cleavage rates were observed for different buffers at the pH-range boundaries indicated above (see Figure 2, below).

Reactions were initiated by the addition of substrate (in H_2O or D_2O) to catalyst in the appropriate buffer salts. Time point aliquots were quenched in 2 volumes of 90% formamide/50 mM EDTA/0.01% bromophenol blue/0.01% xylene cyanol for O-link and nonbridging phosphorothioate substrate cleavage, and in 90% formamide/50 mM Na-PIPES pH 6.5/25 mM EDTA/0.01% bromophenol blue/0.01% xylene cyanol for S-link cleavage. O-link and nonbridging phosphorothioate samples were analyzed by standard 7 M urea/TBE PAGE, and S-link samples were analyzed by 7 M urea/TAE (40 mM Tris acetate/1 mM EDTA, pH 6.7) PAGE.[36] Autoradiography data were processed using Imagequant v5.2. Nonlinear least-squares fits were generated using Sigma Plot. Substrate cleavage data were fit to

$$P = P_0 + P_\infty(1 - e^{k_{obs}t}) \quad (1)$$

where P is the fraction substrate cleaved, P_0 is the initial fraction cleaved, P_∞ is the final fraction cleaved, k_{obs} is the observed first-order rate constant, and t is time. For nonbridging phosphorothioate cleavage experiments, biphasic data were fit to

$$P = P_0 + P_{\infty slow}(1 - e^{k_{slow}t}) + P_{\infty fast}(1 - e^{k_{fast}t}) \quad (2)$$

where a rate constant and final fraction cleaved are determined for each of the two phases (denoted as "fast" and "slow") resulting from the cleavage of the two different cleavage site phosphorothioate diastereomers.

2′-Bromoacetamide Affinity Labeling Experiments. The 2′-bromoacetamide substrate analogue was prepared by specific bromoacetylation of the single 2′-amino group of oligo-**6** by reaction with the *N*-hydroxysuccimidyl ester of bromoacetic acid;[37] this procedure has been described previously.[20] Alkylation reactions conditions were 2.5 μM bromoacetylated oligo-**6**, a trace (<10 nM) of 5′-^{32}P-labeled 9_{25}-11, in the standard reaction buffer at pH 8, at room temperature in the dark. Time point aliquots were quenched with 2 volumes of 90% formamide/50 mM EDTA/0.01% bromophenol blue/0.01% xylene cyanol. Reaction products were analyzed by 15% PAGE and autoradiography as described above. The pH−rate profile reactions were conducted with 3.0 μM bromoacetylated oligo-**6** and 2.5 μM 9_{25}-11 (including a trace of 5′-^{32}P-labeled 9_{25}-11) under standard conditions. As described previously for similar experiments, initial time points (<15% completion) were analyzed by linear regression for the pH−rate profile to avoid the complicating effects of variations in the rate of bromoacetamide solvolysis with changing pH.[21]

Larger scale reactions of 1−2 nmols 9_{25}-11 were carried out for digestion/MALDI analysis under the following conditions: 5 μM 9_{25}-11, 10 μM bromoacetamide substrate analogue, in standard buffer. After ~48 h, reactions were terminated by butanol concentration to ~100 μL, followed by ethanol precipitation. Samples were resuspended in 90% formamide/50 mM EDTA/0.01% bromophenol blue/0.01% xylene cyanol. Alkylated 9_{25}-11 was resolved by preparative 15% PAGE and identified by UV-shadowing. The material was eluted from the gel slice into 1% $LiClO_4$/10 mM Tris-HCl at room temperature after freezing on dry ice. The sample was then concentrated to ~100 μL, precipitated with acetone, dried, resuspended in H_2O, and G-25 desalted. Both alkylated and unreacted 9_{25}-11 were treated with Micrococcal Nuclease (typically 10−20 units) in 1 mM $CaCl_2$/10 mM Tris-HCl pH 8 for varying times (up to 72 h) at 37 °C. Some digestion reactions also included 2 units of shrimp alkaline phosphatase to remove terminal phosphates; this treatment facilitated the observation of larger digestion fragments in MALDI spectra. Digestion progress was surprisingly slow, perhaps due to the modified nucleotide structures and/or the presence of alkylation linkage between the DNAzyme and substrate strands. Progress was monitored by labeling a few picomoles of material from the digestion mixture with γ-^{32}P-ATP and polynucleotide kinase, and then observing the sizes of the labeled fragments resolved by 20% PAGE. Digestion samples were precipitated with 1% $LiClO_4$/acetone or speed-vac concentrated for MALDI analysis. MALDI samples were prepared and spectra recorded as previously described.[20]

Synthesis of the S-link Substrate (Oligo-3). Our general method for synthesizing radiochemical quantities of S-link substrates has been described elsewhere;[27] a brief description is provided here (also see Supporting Information). First, the requisite bridging thiophosphate moiety was introduced at the 5′-end of oligo-**2**. The standard, protected, solid-phase bound oligo-**2** was converted to the 5′-iodide by brief treatment with $[(PhO)_3PCH_3][I]$;[38] the bridging thiophosphate was subsequently introduced by treatment with aqueous Na_3SPO_3.[39] Following NH_4OH deprotection, the desired product was isolated by 20% PAGE purification; the 5′-phosphorylated-oligo-**2** served as a migration standard. The sample was eluted from the gel and stored in 10 mM Na-borate pH 9, where it is reasonably stable to hydrolysis.[40] The identity of the thiophosphate product was confirmed by MALDI mass spectrometry (see Supporting Information). The linkage of the thiophosphate via sulfur to the 5′-carbon of oligo-**2** was confirmed by the observation of rapid dephosphorylation[40] at pH 5 to yield 5′-thiol-oligo-**2** (see Supporting Information).

The S-link substrate (oligo-**3**) was then produced by enzymatic ligation of 5′-thiophosphorylated-oligo-**2** to oligo-**1** using oligo-**5** as a template. The resulting biotinylated duplex was then bound to streptavidin magnetic particles. The solid phase was washed several times to remove unreacted ligation substrates, whereupon the desired S-link substrate (oligo-**3**) was released from the solid phase under mildly denaturing conditions. The sample was then G-25 desalted for immediate use in kinetic experiments (described above). The presence of the bridging phosphorothioate linkage in the S-link substrate (oligo-**3**) was confirmed by rapid and quantitative cleavage in the presence of Ag^+;[26] the native O-link substrate (oligo-**4**) was not affected by this treatment (see Supporting Information).

Results and Discussion

General Properties of 9_{25}-11 Catalysis. Before attempting to chemically probe for 9_{25}-11 functional groups involved in catalysis, we first examined 9_{25}-11 for properties indicative of general acid/base catalysis and similarities to RNaseA. Previous kinetics studies[34] have established that single-turnover (excess catalyst) cleavage of the native substrate (oligo-**4**) by 9_{25}-11 follows well-behaved saturation kinetics under the following conditions: 50 mM Tris-HCl pH 7.5, 200 mM NaCl, 1 mM EDTA. Unless stated otherwise, all experiments reported in this study were performed in the same buffer at ambient temperature (21−22 °C), under single-turnover conditions where substrate was saturated with DNAzyme.

The pH−rate profile for native substrate cleavage by 9_{25}-11 (Figure 2) exhibits a classic bell shape, not dissimilar to that observed for RNaseA catalysis,[41,42] and consistent with general acid/base catalysis. As in the case of RNaseA, the two titratable

(36) Kuimelis, R. G.; McLaughlin, L. W. *Biorg. Med. Chem.* **1997**, *5*, 1051–1061.
(37) Povsic, T. J.; Dervan, P. B. *J. Am. Chem. Soc.* **1990**, *112*, 9428–9430.
(38) Miller, G. P.; Kool, E. T. *Org. Lett.* **2002**, *4*, 3599–3601.
(39) Zhang, B.; Cui, Z.; Sun, L. *Org. Lett.* **2001**, *3*, 275–278.
(40) Dittmer, D. C.; Ramsay, O. B.; Spalding, R. E. *J. Org. Chem.* **1963**, *28*, 1273–1278.
(41) Schultz, L. W.; Quirk, D. J.; Raines, R. T. *Biochemistry* **1998**, *37*, 8886–8898.
(42) del Rosario, E. J.; Hammes, G. G. *Biochemistry* **1969**, *8*, 1884–1889.

catalytic residues exhibit similar pK_a values (7.6 ± 0.1 and 8.4 ± 0.1), although the pK_a values exhibited for 9_{25}-11 catalysis are significantly higher than those reported for RNaseA (reported as 5.4 and 6.4 based on pH−rate profiling,[42] and 5.8 and 6.2 based on NMR titration[43]). The pK_a of 4-methyl-imidazolinium (7.45) serves as a point of reference for the unperturbed pK_a of a 4-alkyl-imidazole functionality that is common to both RNaseA (histidine side chains) and 9_{25}-11 (^{his}dA side chains).[44] Upward perturbation of imidazole pK_a values in the active site of 9_{25}-11 would not be surprising in the negatively charged environment of a nucleic acid structure; conversely, the downward perturbation of the His12 and His119 is consistent with the positive electrostatic potential known to exist in the active site of RNaseA.[46] Therefore, the difference in pK_a values between RNaseA and 9_{25}-11 could be consistent with general acid/base catalysis by a pair of 9_{25}-11 imidazole side chains. In deuterated buffers, the pD−rate profile (Figure 2) mirrors the pH dependence in H_2O buffer, with a strong solvent isotope effect at pL < ~8; also, the apparent pK_a's of the titratable catalytic functionalities are shifted noticeably higher in deuterated buffer. Overall, the pH−rate profile and solvent isotope effect data are consistent with a rate-limiting, general acid/base-catalyzed chemical step in 9_{25}-11 catalysis.

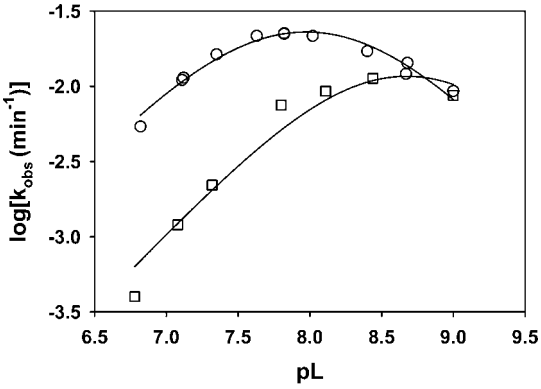

Figure 2. pH−rate (○) and pD−rate (□) profiles for 9_{25}-11-catalyzed cleavage of substrate (oligo-**4**) in standard buffer. The data were fit to a general acid/base catalysis model: $\log k_{obs} = \log (k_{max}/(1 + 10^{pK_{a1}-pH} + 10^{pH-pK_{a2}} + 10^{pK_{a1}-pK_{a2}}))$.[45] The kinetic p$K_a$ values determined were 7.6 ± 0.1 and 8.4 ± 0.1 in H_2O buffers, and 8.4 ± 0.8 and 8.9 ± 1.3 in D_2O buffers.

Next, we focused more specifically on determining the mechanistic roles, if any, of the synthetic functionalities in 9_{25}-11. Initial characterization had demonstrated that 9_{25}-11 activity is undetectable when all of the ^{his}dA and ^{aa}dU residues are simultaneously replaced with natural dA and dT, respectively.[17] In this study we undertook a more detailed structure−activity investigation by removing individual imidazole and cationic amine functionalities one at a time (Figure 3). Individual ^{his}dA residues were replaced with 8-methylamino-dA (rather than natural dA) so as to remove the imidazole moiety while still preserving the 8-methylamino group, which could engage in hydrogen bonding or other functions. Individual ^{aa}dU residues were replaced with natural dT residues so as to remove the cationic amine functionality.

(43) Markley, J. M. *Acc. Chem. Res.* **1975**, *8*, 70–79.
(44) Bruice, T. C.; Schmir, G. L. *J. Am. Chem. Soc.* **1958**, *80*, 148–156.
(45) Bevilacqua, P. C. *Biochemistry* **2003**, *42*, 2259–2265.
(46) Messmore, J. M.; Raines, R. T. *Arch. Biochem. Biophys.* **2000**, *381*, 25–30.

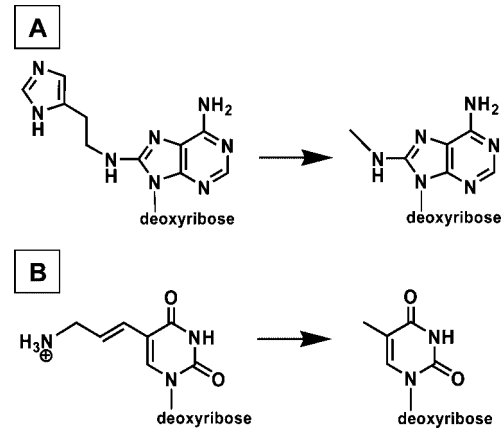

Figure 3. Nucleotide substitutions used in the functional group deletion variants of 9_{25}-11 used in this study: (A) 8-histaminyl-dA (^{his}dA) was replaced with 8-methylamino-dA or (B) 5-aminoallyl-dU (^{aa}dU) was replaced with natural dT.

Cleavage of the native substrate is significantly impaired by the individual deletion of three of the four imidazole groups in 9_{25}-11 (Table 1). Chemical rescue[47] of the 8-methylamino-dA variants (A13, A19, and A23) was attempted using 4-methylimidazole, but no significant rescue of native substrate cleavage activity was observed (data not shown). Notably, the imidazole moiety of the ^{his}dA24 residue appears to be completely dispensable, as its removal actually leads to slight enhancement of catalytic activity. Individual removal of the cationic amine functionalities caused relatively minor (<10-fold) impairment in all cases except for the T21 variant, which was 50-fold less active than wildtype 9_{25}-11. Not surprisingly, it appeared that several of the synthetic appendages, especially imidazole groups, are crucial for proper folding or catalysis in 9_{25}-11, but the question remained whether any of the imidazoles or cationic amines played catalytic roles which mimic the active site mechanism in RNaseA and, if so, which ones. We therefore applied a series of chemical probes to study the mechanism of 9_{25}-11 catalysis in more detail.

Table 1. Effects of Individual Functional Group Deletion on the Observed Rate Constants for 9_{25}-11-Catalyzed Cleavage of the Native (O-Link) and the Bridging Phosphorothioate (S-Link) Substrates in Standard Buffer (pH 7.5)

DNAzyme[a]	k_O (min^{-1})	$k_{O\ rel}$[b]	k_S (min^{-1})	$k_{S\ rel}$[b]	k_O/k_S
WT	0.020	1	0.20	1	10
A13	0.00005	0.0025	0.019	0.095	380
A19	0.00007	0.0035	0.061	0.31	871
A23	<0.00001	<0.00005	0.0017	0.0085	>170
A24	0.045	2.3	0.22	1.1	4.9
T8	0.0074	0.37	0.067	0.34	9.0
T9	0.0068	0.34	0.052	0.26	7.6
T11	0.0025	0.13	0.048	0.24	19
T14	0.0097	0.49	0.086	0.43	8.9
T18	0.012	0.60	0.097	0.49	8.1
T21	0.0004	0.020	0.011	0.055	28
none[c]	n.d.[d]	n.d.[d]	0.00069	0.0035	n.d.[d]

[a] WT (wildtype) refers to the originally selected 9_{25}-11 DNAzyme sequence.[15,17] 9_{25}-11 functional group deletion variants are named to indicate the nucleotide from which the synthetic imidazole or cationic amine functionality was removed. For example, A13 indicates that 8-methylamino-dA has been substituted for the wildtype ^{his}dA at residue 13. [b] k_{rel} is the ratio k(variant)/k(wildtype) for either native (O-link) or S-link substrate cleavage. [c] Background cleavage rate constant in standard buffer (pH 7.5). [d] Not detected.

General Base Catalysis. In order to probe for DNAzyme functional groups involved in general base catalysis, we

employed an affinity labeling approach which was used originally as a probe for general base catalysis in RNaseA[19] and, recently, in two natural ribozymes.[20,21] In this experiment, the nucleophilic 2′-OH at the substrate cleavage site, which would normally be deprotonated by a general base, is replaced with an electrophilic bromoacetamide moiety (Figure 1C). The highly electrophilic 2′-bromoacetamide probe is well positioned to alkylate the DNAzyme general base in particular, to facilitate its identification (Scheme 2).

Scheme 2. Alkylation of a Hypothetical Imidazole General Base by the 2′-Bromoacetamide Affinity Label

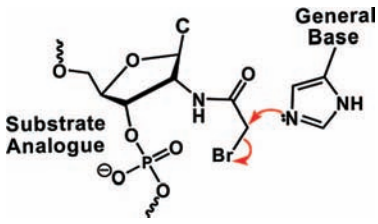

Incubation of the bromoacetamide probe with ^{32}P-labeled 9_{25}-11 indeed yielded a higher molecular weight covalent adduct to 9_{25}-11, as revealed by denaturing PAGE analysis (see Supporting Information). The properties of this alkylation reaction were compared to those of the catalytic reaction (Figure 4A) in order to gauge whether alkylation occurs within a catalytically competent DNAzyme fold. Like the catalytic reaction,[34,35] the alkylation reaction is inhibited by the addition of a noncleavable substrate analogue, which demonstrates that alkylation depends upon normal substrate binding to the DNAzyme. Also as with the catalytic activity,[15] alkylation activity depends upon the presence of NaCl, which suggests that the alkylation reaction reflects the catalytically active DNAzyme conformation. Finally, Hg^{2+} is known to potently inhibit 9_{25}-11 catalysis, [48] and we observe the same dramatic effect upon the alkylation reaction.

The pH dependence of the 9_{25}-11 alkylation reaction (Figure 4B) was also determined to verify that the alkylated nucleophile is a titratable active site residue, and thus a reasonable candidate for general base catalyst. Above pH ~6.5, the increase in alkylation rate appears to reflect titration of the alkylated nucleophile (in analogy to titration of the general base), as it becomes fully deprotonated at pH ~9. Furthermore, the apparent pK_a for the alkylated nucleophile closely matches one of the pK_a's derived from the catalytic pH−rate profile (7.6 ± 0.1 for catalysis versus 7.7 ± 0.1 for alkylation). This correspondence suggests that the alkylated nucleophile could be the same DNAzyme functional group which acts as the general base in the catalytic reaction.

As expected, the alkylation rate does not decrease above pH ~8, as does the catalytic rate, because general acid deprotonation

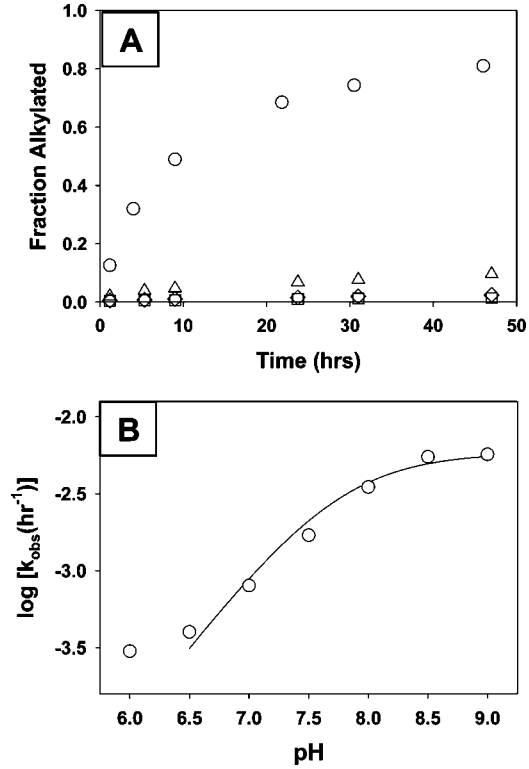

Figure 4. Effects of reaction conditions on the 9_{25}-11 affinity labeling reaction. (A) Alkylation reactions were carried out under standard conditions (pH 7.5) (○), in the absence of NaCl (△), in the presence of 0.5 mM Hg^{2+}(□), and in the presence of 10 μM 2′-amino substrate analogue (oligo-**6**) (◇). All reactions were carried out in standard buffer (pH 7.5) with the noted changes; data were fit to eq 1. (B) Alkylation reaction pH−rate profile in standard buffer. Data were fit to log $k_{obs} = \log(k_{max}/(1 + 10^{pK_a - pH}))$, which yielded p$K_a = 7.7 \pm 0.1$ (data for pH 6 were not included in the fit, as explained in the text).

is inconsequential for the general base alkylation reaction, whereas general acid deprotonation inhibits the catalytic reaction. Also, contrary to the continued titration of the general base expected at lower pH, alkylation activity levels off below pH ~7. This effect has been observed previously in the hammerhead ribozyme, where guanosine N1 alkylation was pH-independent below pH ~7; this unexpected result was attributed to a basal, pH-independent alkylation mechanism (perhaps akin to an electrophilic aromatic substitution mechanism) which overwhelms the pH-dependent mechanism as the nucleophile becomes largely protonated at lower pH.[21] Overall, the 9_{25}-11 alkylation reaction appears to reflect the properties of the catalytic reaction, which suggests that 2′-bromoacetamide affinity labeling offers relevant mechanistic insight into general base catalysis.

In previously reported ribozyme affinity labeling experiments,[20,21] alkylation lesions on the ribozyme strand were readily identified by alkaline footprinting; this approach is impossible for a DNAzyme given the relative stability of DNA at high pH. As an alternative, hydroxyl radical and DNaseI footprinting were attempted, but neither approach yielded clear results (data not shown). Purine N3 or N7 alkylation lesions in DNA, which induce depurination,[49] can be located with hot piperidine treatment, which affords cleavage of the abasic site. Of note, the 9_{25}-11 alkylation linkage was completely stable to

(47) Examples of chemical rescue experiments for nucleic acid catalysts (a) Peracchi, A.; Beigelman, L.; Usman, N.; Herschlag, D. *Proc. Natl. Acad. Sci. U.S.A.* **1996**, *93*, 11522–11527. (b) Peracchi, A.; Matulic-Adamic, J.; Wang, S.; Beigelman, L.; Herschlag, D. *RNA* **1998**, *4*, 1332–1346. (c) Perrotta, A. T.; Shih, I.-H.; Been, M. D. *Science* **1999**, *286*, 123–126. (d) Lebruska, L. L.; Kuzmin, I. I.; Fedor, M. J. *Chem. Biol.* **2002**, *9*, 465–473. (e) Kuzmin, Y. I.; Da Costa, C. P.; Fedor, M. J. *J. Mol. Biol.* **2004**, *340*, 233–251. (f) Kuzmin, Y. I.; Da Costa, C. P.; Cottrell, J. W.; Fedor, M. J. *J. Mol. Biol.* **2005**, *349*, 989–1010. (g) Perrotta, A. T.; Wadkins, T. S.; Been, M. D. *RNA* **2006**, *12*, 1282–1291.

(48) Thomas, J. M.; Ting, R.; Perrin, D. M. *Org. Biomol. Chem.* **2004**, *2*, 307–312.

(49) Gates, K. S. In *Reviews of Reactive Intermediate Chemistry*; Platz, M. S., Moss, R. A., Jones, M., Eds.; John Wiley & Sons, Inc.: New York, 2007; pp 337−339.

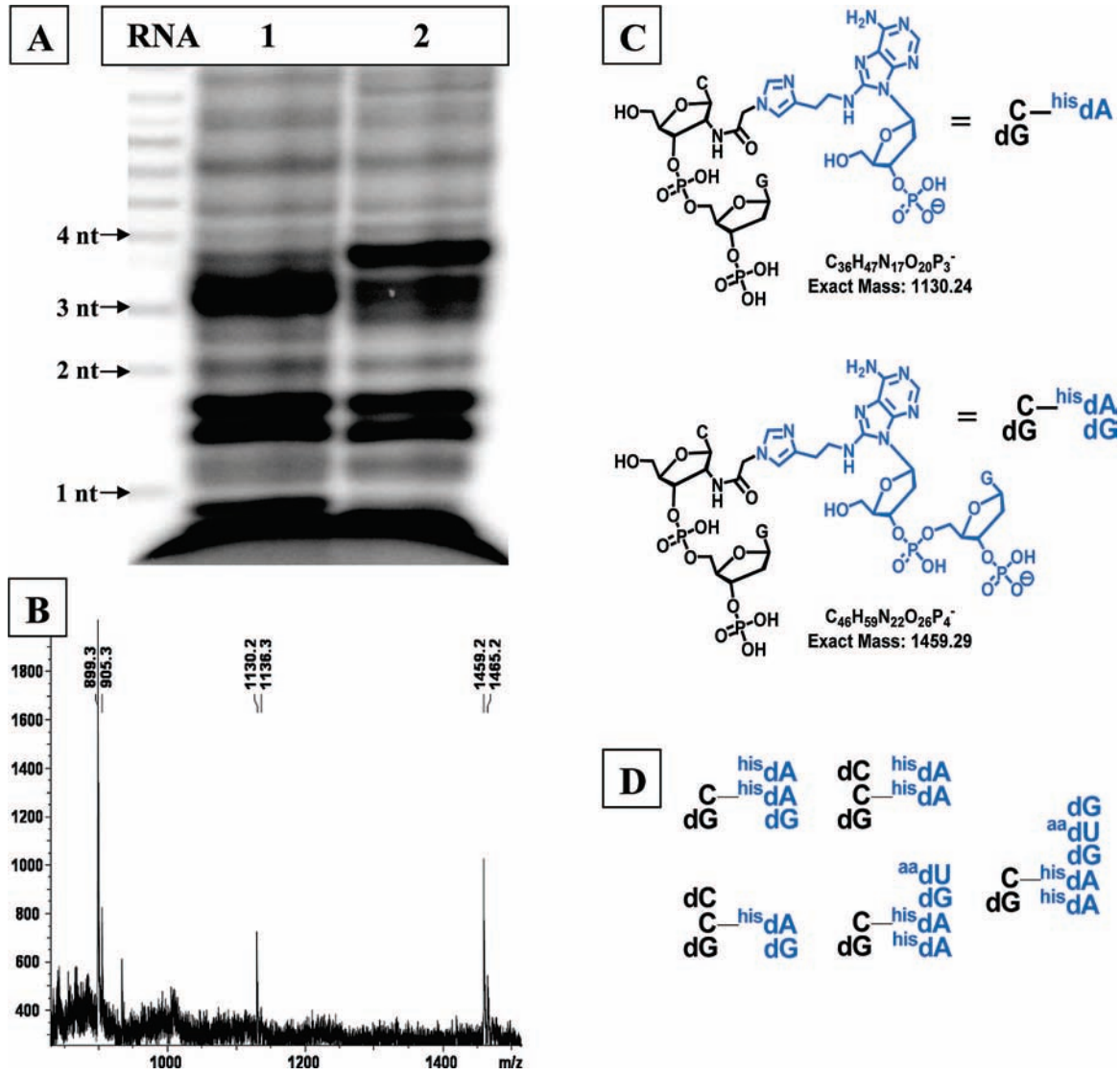

Figure 5. (A) 20% PAGE analysis following ^{32}P-labeling of fragments resulting from exhaustive nuclease digestion of unreacted 9_{25}-11 and oligo-**6** (lane 1) and purified alkylated 9_{25}-11 (lane 2). An RNA cleavage ladder is labeled at left to help gauge the digestion fragment sizes. (B) MALDI spectrum obtained for the alkylated catalyst digestion sample analyzed in panel A. The fragment with $m/z = 899.3$ is assigned to the sequence 5′-TpGpG (predicted $m/z = 899.2$), which corresponds to the 3′-terminus of the affinity label sequence (oligo-**6**). Signals corresponding to +6 m/z units correspond to Li^+ adducts (sample preparation included $LiClO_4$ precipitation). (C) Proposed structures of fragments assigned in panel B which contain the alkylation linkage. Nucleotides derived from the affinity label are black, and nucleotides derived from 9_{25}-11 are blue. (D) Fragments containing the alkylation linkage observed after less extensive digestion (see Supporting Information). Linkage to the imidazole group of ^{his}dA23 is assigned on the basis of functional group deletion data (Figure 6) and the piperidine stability of the alkylation linkage (see text and Supporting Information).

hot piperidine treatment (see Supporting Information), thus ruling out purine alkylation at the nucleophilic N3 or N7 positions (purine N1 alkylation cannot be ruled out, as these lesions do not cause significant depurination).[49] In order to more precisely identify the DNAzyme alkylation site, the alkylated DNAzyme was submitted to enzymatic digestion followed by mass spectrometric fragment analysis.

For mass spectrometric analysis, the alkylation reaction was performed on larger scale (1−2 nmols 9_{25}-11), and the cross-linked product was isolated by preparative PAGE and subjected to nuclease digestion. The digestion progress could be monitored by ^{32}P-labeling the resulting fragments and judging their size distribution by PAGE analysis. For example, Figure 5A shows the results for a sample of alkylated 9_{25}-11 subjected to exhaustive nuclease digestion compared with a similarly digested mixture of unreacted 9_{25}-11 and 2′-amino substrate analogue (oligo-**6**); clearly, different fragments appear in the presence or absence of the alkylation linkage. Figures 5C and 5D summarize the assignments of the digestion fragments observed by MALDI which include the alkylation lesion (all observed fragments are given in the Supporting Information). The sequence assignments of the observed alkylation fragments are consistent with alkylation cross-linking of one of, or both of, ^{his}dA23 and ^{his}dA24; these possibilities cannot be distinguished on the basis of the MADLI data. All alkylation fragments also contain at least one dG residue, which is assigned to the substrate analogue strand, as the nuclease appears to be unable to remove the nucleotide at the 3′-side of the 2′-acetamide-linked substrate nucleotide (this same effect was observed in a ribonuclease digestion experiment with alkylated hairpin ribozyme[20]).

To address which of ^{his}dA23 and ^{his}dA24 had been alkylated, and whether the alkylation linkage involved an imidazole side chain, affinity labeling was performed for all 9_{25}-11 imidazole deletion variants. The rate and extent of 9_{25}-11 alkylation was

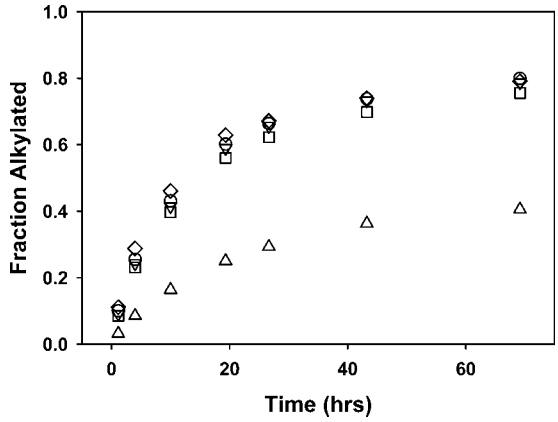

Figure 6. Alkylation of imidazole deletion variants of 9_{25}-11 in standard buffer at pH 7.5. The fraction of DNAzyme alkylated is plotted as a function of time for wildtype 9_{25}-11 (◇) and the A13 (○), A19 (▽), A23 (△), and A24 (□) imidazole deletion variants.

significantly diminished only when the imidazole side chain of ^{his}dA23 was absent, in the A23 variant (Figure 6). This finding suggests that alkylation occurs at least primarily on the imidazole moiety of ^{his}dA23 in wildtype 9_{25}-11; therefore, this functional group appears to be positioned similarly to the His12 general base in RNaseA, which was likewise identified by alkylation.[19] The remaining alkylation activity observed for the A23 variant could result from promiscuous alkylation of the adjacent, catalytically dispensable imidazole side chain of the ^{his}dA24 residue. The alkylation product of the A23 variant showed no significant difference in PAGE mobility relative to wildtype alkylation product, which would indicate the existence of an alternative alkylation linkage in the A23 variant. It is not surprising, however, that the products resulting from the alkylation of adjacent DNAzyme nucleotides would be electrophoretically indistinguishable; previous alkylation of the hammerhead ribozyme yielded four different alkylation linkages to four consecutive residues, all of which were inseparable by high-resolution PAGE.[21]

The data from the digestion/mass spectrometry and imidazole deletion experiments, along with the noted stability of the alkylation lesion to hot piperidine treatment, strongly support the assignment of the DNAzyme alkylation site to the imidazole side chain of the ^{his}dA23 residue. The correlation of the properties of the alkylation and catalytic reactions provides strong evidence that this functional group acts as a general base in the 9_{25}-11 catalytic mechanism. Moreover, the results for 9_{25}-11 directly parallel the results of the analogous affinity labeling study of RNaseA in which the general base catalyst (the His12 imidazole side chain) was alkylated by 2′-bromoacetamido mononucleotides; this obvious parallel suggests that 9_{25}-11 and RNaseA share a similar imidazole-mediated general base catalysis mechanism.

General Acid Catalysis. Bridging phosphorothioate (S-link) substrates (Figure 1C) have proven useful for identifying active site functional groups involved in general acid catalysis in both protein[23−25] and ribozyme[26,27]-catalyzed phosphodiester transfer reactions. The more labile departure of the lower pK_a sulfur leaving group in the course of S-link substrate cleavage is known to proceed without benefit from acid catalysis;[22] therefore, catalyst mutations that impair general acid catalysis should significantly impair native (O-link) substrate cleavage, but should have negligible effects on S-link cleavage.[23−27] Conversely, mutations which impair aspects of catalysis other than general acid catalysis should affect activity against the O-link and S-link substrates to a similar degree. Thus, catalyst functional groups which contribute specifically to general acid catalysis can be identified on the basis of which mutations, or functional group deletions, lead to a conspicuously large ratio of rate constants for S-link and O-link substrate cleavage (k_S/k_O) relative to wildtype.[26,27]

The rate constants for single-turnover cleavage of O-link and S-link substrates, along with corresponding k_S/k_O values, for wildtype and variant 9_{25}-11 DNAzymes are compared in Table 1. The largest k_S/k_O value (87 times that observed for wildtype 9_{25}-11) was observed upon removal of the imidazole side chain of ^{his}dA19, which suggests its involvement in general acid catalysis. This result directly parallels the findings of a related study of RNaseA: Thompson and Raines showed that the H119A mutation significantly impairs RNaseA activity against native RNA substrates, but has relatively little effect on activity against a substrate with a lower pK_a nitrophenolate leaving group.[3] These results provided convincing evidence that implicated His119 acts as a general acid by protonating the substrate leaving group in RNaseA catalysis. Similarly, S-link substrates have been used in conjunction with active site mutation to identify functional groups involved in general acid catalysis in the HDV[26] and hammerhead[27] ribozymes, as well as in phospholipase enzymes, which catalyze an intramolecular phosphodiester transfer similar to RNA cleavage.[23−25]

Although not as large as that for the A19 variant, the k_S/k_O value observed for the A13 variant is still conspicuously greater than that for wildtype 9_{25}-11. This indicates that the ^{his}dA13 imidazole is also important for efficient general acid catalysis, although less so than the ^{his}dA19 imidazole. Similar restoration of activity against S-link substrates has been observed before for the mutation of active site residues other than the putative general acid in both a protein enzyme[23,24] and a ribozyme.[27] In the case of a phospholipase enzyme, the additionally identified residue is thought to engage in hydrogen-bonding interactions that are important for the proper alignment of the general acid for proton transfer to the substrate.[23,24] Similarly, mutations to the hammerhead ribozyme active site which disrupt crucial active site hydrogen bonds elicited large k_S/k_O values, indicating the importance of these interactions for proper structuring of the general acid residue.[27] It is possible that the ^{his}dA13 imidazole may contribute similarly to proper positioning of the ^{his}dA19 imidazole for proton transfer to the leaving group, although in the absence of structural data its role remains unclear. A similar interaction has been suggested in RNaseA based on crystallographic and biochemical data, wherein the carboxylate side chain of Asp121 appears to hydrogen bond to His119, which is hypothesized to favor the tautomer which is most productive for general acid catalysis.[41,50]

The A23 9_{25}-11 variant also exhibited a rather large k_S/k_O value relative to wildtype 9_{25}-11, which was not expected given that the ^{his}dA23 imidazole is implicated in general *base* catalysis (*vide supra*). A similar effect was noted in the hammerhead ribozyme, where mutation of the putative general base (G12) gave a significant k_S/k_O value; this result was attributed to the fact that general base mutation disrupts crucial active site hydrogen bonds and causes structural misplacement of the general acid. In the case of the A23 9_{25}-11 variant, the rate constant for S-link substrate cleavage, however, is just 3-fold

(50) Quirk, D. J.; Park, C.; Thompson, J. E.; Raines, R. T. *Biochemistry* **1998**, *37*, 17958–17964.

greater than the background cleavage rate constant (Table 1); such a minor degree of rate enhancement could result from structural constraints in the substrate−DNAzyme complex which might favor the in-line nucleophilic attack geometry required in RNA cleavage.[51] Overall, the S-link substrate cleavage data suggest that the imidazole side chain of ^{his}dA19 mediates general acid catalysis in 9_{25}-11, with direct analogy to the mechanistic role of His119 in RNaseA. The imidazole side chain of ^{his}dA13 also appears to play a less direct role in facilitating general acid catalysis.

DNAzyme−Scissile Phosphate Interactions. In RNaseA catalysis, the cationic amine functionality of Lys41 is believed to provide hydrogen bond stabilization for the accumulation of negative charge on the nonbridging oxygens in the pentacoordinate phosphorane transition state/intermediate.[2,4] To probe for similar interactions in 9_{25}-11 catalysis, we examined the cleavage of a nonbridging phosphorothioate substrate (Figure 1C) in the context of DNAzyme functional group removal. The nonbridging sulfur substitution alters the electronic and hydrogen-bonding properties of the scissile phosphate; therefore, we hypothesized that this substitution should significantly affect catalysis by altering any DNAzyme−transition state interaction(s) involving the scissile phosphate nonbridging oxygen(s). Furthermore, in 9_{25}-11 variants in which this interaction is absent or disrupted, we expected that (1) cleavage of the native substrate should be significantly impaired, and (2) cleavage of the nonbridging phosphorothioate substrate should be very similar to native substrate, as observed for base-catalyzed phosphorothioate cleavage.[28,52] In contrast, for 9_{25}-11 variants in which the DNAzyme−scissile phosphate interaction remains intact, cleavage of the nonbridging phosphorothioate substrate should be significantly impaired relative to the native substrate.

In our experiments, we used the (∼50:50) mixture of cleavage site phosphorothioate diastereomers which results from the standard sulfurization reaction in solid-phase synthesis.[53] Kinetic data for carbonate-induced cleavage of the phosphorothioate substrate mixture fit very well to a monophasic model (R^2 = 0.9982) (see Supporting Information), which indicates that nonenzymatic, base-catalyzed cleavage of the two diastereomers proceeds through transition states which are nearly energetically indistinguishable (this has been demonstrated for different RNA sequences[52] and has also been predicted theoretically[54]). In contrast, cleavage of this diastereomeric mixture catalyzed by wildtype 9_{25}-11, and all but one of the variants tested (*vide infra*), was clearly biphasic (Figure 7B and Supporting Information). This clear difference confirms that the biphasic nature of 9_{25}-11-catalyzed phosphorothioate cleavage results from diastereoselectivite DNAzyme−scissile phosphate interaction(s), and not from intrinsic transition-state energy differences inherent in the cleavage of the two substrate diastereomers (at least where nonbridging oxygen negative charge is not stabilized by protonation, as in the specific base catalyzed mechanism, which predominates at pH > ∼5[59]).

In 9_{25}-11-catalyzed nonbridging phosphorothioate cleavage, the rate of the faster cleaving phase is not significantly affected relative to native substrate cleavage for wildtype 9_{25}-11 and all variants tested (Table 2). Thus, the fast phase likely reflects cleavage of the substrate diastereomer in which the sulfur substitution exerts little effect on the scissile phosphate−DNAzyme interaction(s). The slower phosphorothioate cleavage phase proceeds roughly 10-fold more slowly than native substrate cleavage for all of the 9_{25}-11 variants for which a slow cleaving phase was detected. Thus, the slower cleaving phase represents cleavage of the phosphorothioate diastereomer where the nonbridging sulfur atom disrupts interactions between the scissile phosphate and 9_{25}-11. This analysis required us to analyze rate constants, often under biphaisic kinetics, as well as end points (P_∞) defined as the fraction cleaved at $t = \infty$, as determined by fitting the data to eq 1 or 2.

For all of the variants except for T21, the fast phosphorothioate cleavage phases exhibited end points approximately half the size of those for native substrate cleavage; likewise, the slow phosphorothioate cleavage phases all exhibited end points less than half the size of those for native substrate cleavage. In contrast, the T21 variant exhibited monophasic cleavage of the phosphorothioate mixture (Figure 7). Furthermore, the T21 variant cleaved *more than half* of the phosphorothioate substrate mixture, and to nearly the same end point as for native substrate cleavage by the T21 variant (Table 2). Thus, the single phosphorothioate cleavage phase observed for the T21 variant comprises the cleavage of both substrate diastereomers at indistinguishable rates.

In the case of the T21 variant, the fact that the two diastereomers of the nonbridging phosphorothioate substrate are cleaved at indistinguishable rates, which are also similar to the rate of native substrate cleavage, suggests that the cationic amine side chain of ^{aa}dU21 is responsible for the diastereoselective interaction with a nonbridging scissile phosphate oxygen. In the case of the aforementioned phospholipase, similar reasoning has been used, in light of crystal structure data, to verify the diastereoselective interaction of an arginine side chain with substrate nonbridging phosphate oxygens: in that case, arginine mutation completely abolished a 7600-fold rate difference for the cleavage of the two substrate diastereomers by the wildtype enzyme.[55]

The magnitude of the nonbridging thio-effects has also been used to distinguish between transition-state stabilization of a pentacoordinate phosphorane by full protonation of a nonbridging oxygen (in a "triester-like" mechanism[56]), or by electrostatic and hydrogen-bond-type interactions (a "classical" mechanism).[24,28,57] At low pH, full protonation of nonbridging oxygens via specific acid catalysis is well characterized in the cleavage of RNA model systems,[58] and under these conditions, nonbridging phosphorothioate substitution is known to diminish cleavage rate by factors of 100 or more.[29,58] In contrast, nonbridging phosphorothioate substitution has very little effect on specific base-catalyzed RNA cleavage, where nonbridging

(51) Soukup, G. A.; Breaker, R. R. *RNA* **1999**, *5*, 1308–1325.
(52) (a) Burgers, M. J.; Eckstein, F. *Biochemistry* **1979**, *18*, 592–596. (b) Herschlag, D.; Piccirilli, J. A.; Cech, T. R. *Biochemistry* **1991**, *30*, 4844–4854. (c) Almer, H.; Stromberg, R. *Tetrahedron Lett.* **1991**, *32*, 3723–3726.
(53) (a) Wilk, A.; Stec, W. J. *Nucleic Acids Res.* **1995**, *23*, 530–534. (b) Dr. Richard Pon, University of Calgary DNA Services, personal communication.
(54) (a) Gregersen, B. A.; Lopez, X.; York, D. M. *J. Am. Chem. Soc.* **2003**, *125*, 7178–7179. (b) Gregersen, B. A.; Lopez, X.; York, D. M. *J. Am. Chem. Soc.* **2004**, *126*, 7504–7513.
(55) Kravchuk, A. V.; Zhao, L.; Kubiak, R. J.; Bruzik, K. S.; Tsai, M.-D. *Biochemistry* **2001**, *40*, 5433–5439.
(56) Breslow, R.; Xu, R. *Proc. Natl. Acad. Sci. U.S.A.* **1993**, *90*, 1201–1207.
(57) Ora, M.; Linjalahti, H.; Lönnberg, H. *J. Am. Chem. Soc.* **2005**, *127*, 1826–1832.
(58) (a) Oivanen, M.; Schnell, R.; Pfleiderer, W.; Lönnberg, H. *J. Org. Chem.* **1991**, *56*, 3623–3628. (b) Jarvinen, P.; Oivanen, M.; Lönnberg, H. *J. Org. Chem.* **1991**, *56*, 5396–5401. (c) Chandler, A. J.; Kirby, A. J. *J. Chem. Soc., Chem. Commun.* **1992**, 1769–1770.

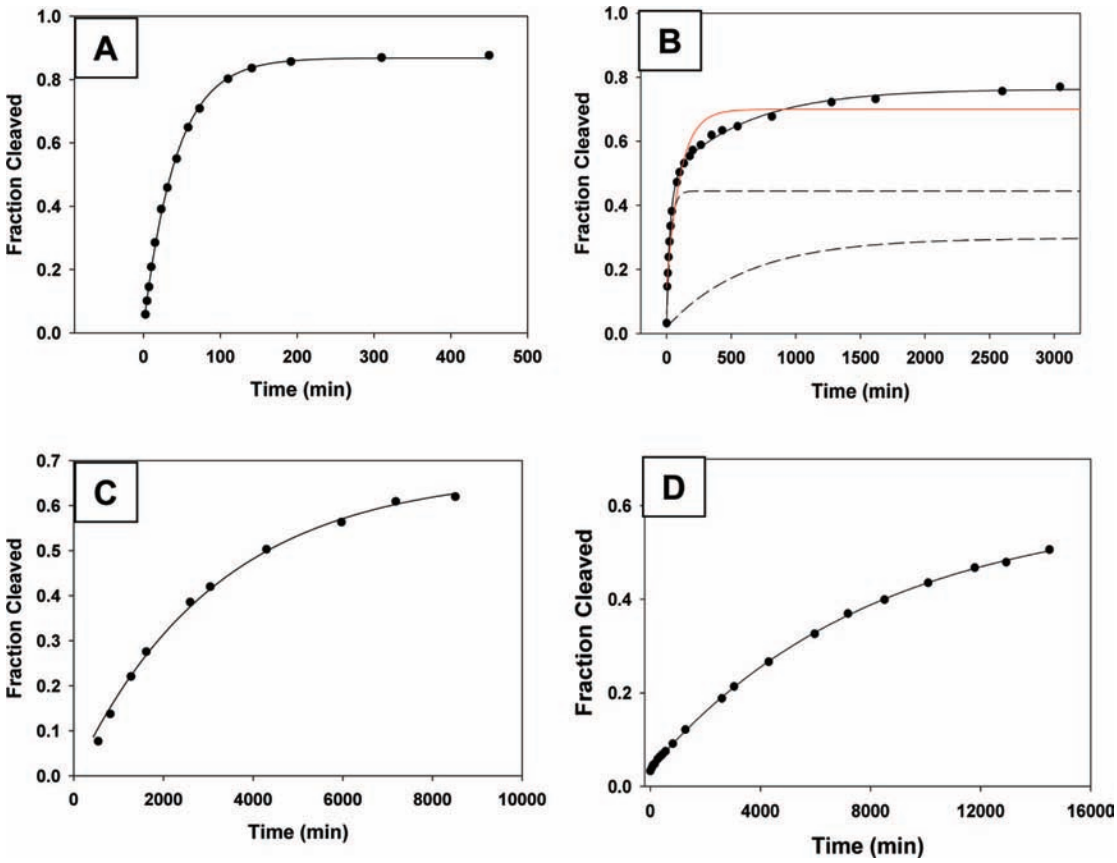

Figure 7. (A) Cleavage of the native substrate by wildtype 9_{25}-11 was monophasic (fit to eq 1, $R^2 = 0.9982$). (B) Wildtype 9_{25}-11 cleavage of the nonbridging phosphorothioate substrate (diastereomeric mixture) is clearly biphasic (fit to eq 2, solid black line, $R^2 = 0.9975$); the two constituent phases are also shown (dashed black lines), and the monophasic fit is shown in red (fit to eq 1, $R^2 = 0.9445$). (C) Cleavage of the native substrate by the T21 variant (fit to eq 1, $R^2 = 0.9996$). (D) Cleavage of the diastereomeric mixture of phosphorothioate substrates by the T21 variant (fit to eq 1, $R^2 = 0.9999$). All reactions were performed in standard buffer at pH 7.5. Similar plots are given in the Supporting Information for the other 9_{25}-11 variants in Table 2.

Table 2. Kinetic Parameters for 9_{25}-11-Catalyzed Cleavage of the Nonbridging Phosphorothioate Substrate (~50:50 Diasteromeric Mixture) in Standard Buffer at pH 7.5[a]

DNAzyme[b]	$k_{S\text{-fast}}/k_O$	$k_{S\text{-slow}}/k_O$	$P_{\infty S\text{-fast}}$	$P_{\infty S\text{-slow}}$	$P_{\infty O}$
WT	1.7	0.1	0.41	0.28	0.86
T8	0.89	0.1	0.45	0.23	0.85
T9	1.7	0.2	0.41	0.24	0.87
T11	0.77	0.07	0.40	0.27	0.80
T14	1.3	0.08	0.46	0.23	0.86
T18	0.81	0.1	0.44	0.30	0.82
T21	0.60	n.d.[c]	0.57	n.d.[c]	0.62

[a] k_O is the observed rate constant for native substrate cleavage and $k_{S\text{-fast}}$ and $k_{S\text{-slow}}$ are the observed rate constants for the fast and slow phases, respectively, of nonbridging phosphorothioate cleavage. The endpoints (P_∞) for each of the phosphorothioate cleavage phases and that for native substrate are also compared. R^2 values are compared for monophasic and biphasic fits of all reactions in the Supporting Information. [b] 9_{25}-11 functional group deletion variant DNAzymes are named as described for Table 1. [c] n.d. = a slow phase was not detected in this reaction.

oxygens remain deprotonated.[59] Therefore, large nonbridging thio-effects in enzyme-catalyzed phosphoryl-transfer reactions have been suggested to indicate a triester mechanism where a nonbridging oxygen atom is fully protonated by an active site residue.[28] For example, phospholipase (wildtype) catalysis was diminished by factors of 10^5 and 4 for the two diastereomeric phosphorothioate substrates relative to the native substrate, which was taken to indicate a triester mechanism in which the *pro-S* oxygen, specifically, is protonated.[24] In contrast, RNaseA catalysis is diminished by factors of 70 and 2 for the two phosphorothioate isomers.[30] This smaller nonbridging thio-effect argues against a triester mechanism in the case of RNaseA;[28] alternatively, Lys41 is thought to stabilize the anionic transition state via hydrogen bond donation to a nonbridging scissile phosphate oxygen.[4,60] Similarly, negligible nonbridging thio-effects have been observed for model systems which involve intramolecular hydrogen bond stabilization (by a hydroxyl group) of negative charge on the nonbridging oxygens.[61] Phosphorothioate substitution also has a minor effect on 9_{25}-11 catalysis (<10-fold), which is consistent with the involvement of the cationic amine side chain of ^{aa}dU21 in a similar hydrogen-bonding and/or Coulombic interaction with the scissile phosphate.

Concluding Remarks

The 9_{25}-11 DNAzyme is the first sequence-specific synthetic RNaseA mimic capable of moderately efficient M^{2+}-independent multiple catalytic turnover ($k_{cat}/K_m \approx 5 \times 10^5$ M^{-1} min^{-1}), a trait that distinguishes it both from all other synthetic constructs that have been generated by rational design as well as from all

(59) (a) Ora, M.; Oivanen, M.; Lönnberg, H. *J. Org. Chem.* **1997**, *62*, 3246–3253. (b) Oivanen, M.; Ora, M.; Almer, H.; Stromberg, R.; Lönnberg, H. *J. Org. Chem.* **1995**, *60*, 5620–5627.

(60) Gerlt, J. A.; Gassman, P. G. *Biochemistry* **1993**, *32*, 11943–11952.

(61) Lönnberg, T.; Ora, M.; Virtanen, S.; Lönnberg, H. *Chem. Eur. J.* **2007**, *13*, 4614–4627.

combinatorially selected nucleic acid catalysts. Such distinctions notwithstanding, in 9_{25}-11, synthetically added, protein-like functionalities are incorporated into a familiar 2D-anatomy resembling the minimal hammerhead ribozyme and 10-23 DNAzyme; therefore, 9_{25}-11 bridges natural nucleic acid catalysts and synthetic ribonuclease mimics.

In this study, we have utilized a broad range of chemical probing and enzymological experiments to investigate the catalytic mechanism of the 9_{25}-11 DNAzyme. The methods used were inspired by analogous experiments used previously to characterize the catalytic mechanisms of RNaseA and natural RNA cleaving ribozymes. In particular, the results of our affinity labeling and bridging phosphorothioate substrate experiments highlight remarkable parallels between the characteristics of RNaseA and 9_{25}-11 catalysis; that is, in both cases specific imidazole groups are implicated in general acid and base catalysis. We have also found strong evidence that a particular cationic amine of 9_{25}-11 interacts diastereoselectively with a nonbridging scissile phosphate oxygen, reminiscent of the role of Lys41 in RNaseA catalysis. However, in the absence of structural data, we cannot rule out other mechanistic possibilities including more complex proton-transfer processes (such as those implicated in buffer-catalyzed mechanisms)[62] or the involvement of active site water molecules in catalysis.[63]

The presence of the synthetic, "RNaseA-like" functionality in 9_{25}-11 provides a significant catalytic advantage compared to unmodified nucleic acid catalysts at physiological pH and ionic strength, in the absence of a M^{2+}-cofactor;[64] however, the catalytic power of 9_{25}-11 still falls far short of that of RNaseA (the value of k_{cat} for RNaseA[3] is some 10^4-10^5-fold greater than k_{cat} for 9_{25}-11). Although this work provides compelling evidence that certain 9_{25}-11 side chains mimic the mechanistic roles of their counterparts in the active site of RNaseA, clearly the organization of these catalytic functional groups in 9_{25}-11 is not optimized to the degree to which evolution has optimized the active site of RNaseA. The *in vitro* evolution of a DNAzyme active site with improved RNaseA-like activity is likely to come from optimization of the *in vitro* selection methodology as well as the inclusion of different and/or additional modified nucleotides. Indeed, toward these ends, we have recently reported a self-cleaving DNAzyme that includes a guanidine functionality.[65]

Our findings demonstrate that supplying appropriate chemical functionality in the context of a combinatorial DNAzyme selection experiment can result in biomimetic catalysts that functionally differ from unmodified nucleic acid catalysts selected to catalyze similar reactions. In this case, it appears that the evolutionary demand for RNA cleavage in the absence of a M^{2+} has been met by deploying active site functional groups which mimic those found at the active site of RNaseA. Thus the addition of synthetic, protein-like functionality has, at least in the case of 9_{25}-11, expanded the diversity of mechanistic strategies available to a nucleic acid-based catalyst.

Acknowledgment. The authors gratefully acknowledge Dr. Leonard Lermer for synthesizing the modified nucleotide phosphoramidites and for helping with initial MALDI experiments. We also thank Prof. Stephen G. Withers for helpful discussions. This work was funded by NSERC, CIHR, and UBC start-up funding. Salary support was provided by NSERC CGS-D and Gladys Estella Laird fellowships (J.M.T.) and a Michael Smith Foundation Senior Career Award (D.M.P.).

Supporting Information Available: Figures S1−S7 and Table S1. This material is available free of charge via the Internet at http://pubs.acs.org.

JA900125N

(62) Lönnberg, T.; Lönnberg, H. *Curr. Opin. Chem. Biol.* **2005**, *9*, 665–673.

(63) (a) Rhodes, M. M.; Reblova, K.; Sponer, J.; Walter, N. G. *Proc. Natl. Acad. Sci. U.S.A.* **2006**, *103*, 13380–13385. (b) Salter, J.; Krucinska, J.; Alam, S.; Grum-Tokars, V.; Wedekind, J. E. *Biochemistry* **2006**, *45*, 686–700. (c) Walter, N. G. *Mol. Cell* **2007**, *28*, 923–929. (d) Torelli, A. T.; Krucinska, J.; Wedekind, J. E. *RNA* **2007**, *13*, 1052–1070. (e) Martick, M.; Lee, T.-S.; York, D. M.; Scott, W. G. *Chem. Biol.* **2008**, *15*, 332–342.

(64) RNA cleavage catalysis is compared for 9_{25}-11 versus unmodified nucleic acid catalysts in more detail in refs 15 and 34.

(65) Hollenstein, M.; Hipolito, C. J.; Lam, C. H.; Perrin, D. M. *Nucleic Acids Res.* **2009**, *37*, 1638–1649.